We are IntechOpen, the world's leading publisher of Open Access books Built by scientists, for scientists

4,800
Open access books available

122,000
International authors and editors

135M
Downloads

Our authors are among the

154
Countries delivered to

TOP 1%
most cited scientists

12.2%
Contributors from top 500 universities

CLARIVATE ANALYTICS BOOK CITATION INDEX INDEXED

WEB OF SCIENCE™

Selection of our books indexed in the Book Citation Index in Web of Science™ Core Collection (BKCI)

Interested in publishing with us?
Contact book.department@intechopen.com

Numbers displayed above are based on latest data collected.
For more information visit www.intechopen.com

Chapter 8

Fiber Bragg Grating Technology for New Generation Optical Access Systems

Oskars Ozolins, Vjaceslavs Bobrovs, Jurgis Porins and Girts Ivanovs

Additional information is available at the end of the chapter

http://dx.doi.org/10.5772/52911

1. Introduction

Thanks to achievements in photonics technologies optical networks have gained a notably increase in capacity per single fiber during the last decade [1]. Demand for greater transmission speed has been increasing exponentially because of the impulsive spread of Internet services (see Fig. 1) [2]. At the same time, the radical improvement of the capability of digital technologies has made feasible expanding multimedia services [1]. Therefore bandwidth intensive applications and exponential Internet traffic growth are continuing to drive the further penetration of optical fiber into the optical access systems [2].

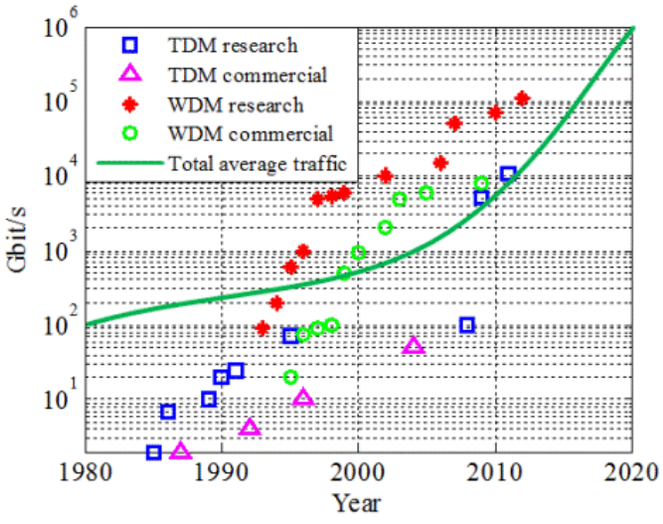

Figure 1. System capacity (per fiber) and network traffic [3]

A new generation access network becomes indispensable to upgrade the systems [4, 5]. The passive optical network (PON) has the feasibility to lead the deployment of new high-

capacity and future-proof broadband networks [6]. The use of wavelength division multiplexing (WDM) in the access networks is further defensible in terms of video services support. WDM solutions are forging ahead towards higher data transmission rate and lower channel spacing to utilize available bandwidth more effectively [7].

The main reasons behind the implementation of new generation systems are to meet demand of capacity, user density requirements and scalability, while ensuring that the cost per unit bandwidth is lowest possible [3, 8]. The novel concept is WDM-direct in which multiple wavelengths are directly connected to each optical network unit (ONU) [9, 10]. Increasing spectral efficiency is important for building efficient WDM-direct systems, since this allows the optical infrastructure to be shared among many channels, and thus reduces the cost per transmitted information bit in a fully loaded system [11]. High performance optical filters are groundwork for realization of high speed dense WDM (DWDM)-direct systems where coherent and incoherent crosstalk between adjacent channels becomes a main source of degradation: adjacent channels interfere with each other upon detection, and the resulting beating gives rise to signal distortions, provided that the beat frequencies lie within the bandwidth of the detection electronics [12, 11].

Proposed approach for increasing the transmission capacity is to reduce the channel spacing of a DWDM-direct system to the minimum while keeping the mature and well developed optical filter technologies like fiber Bragg grating (FBG). To realize proposed approach limitating factors must be taken into account. One part of these factors is related to efficient bandwidth of FBG which in proposed approach is determined employing optical signals (transmission speed 2.5 Gbit/s and 10.3125 Gbit/s which conform 2 Gigabit Ethernet (GE) and 10 GE of Ethernet hierarchy) with different wavelength offset value within filter pass-band. Other part of factors is related to evaluation of the minimal channel spacing for concrete FBG in DWDM-direct system.

2. Optimal complex tranfer function for access systems

A FBG is periodic variation of the refractive index along the propagation direction in the core of optical fiber that reflects particular wavelengths of light and transmits all others. Low channel spacing and high data transmission rate sets strict requirements for DWDM filter characteristics and any imperfections in their parameters, such as amplitude and phase responses, becomes critical. Understanding and distracting of those optical filter imperfections to high speed DWDM-direct systems are of great importance [7].

Low channel isolation from adjacent channels is one of these imperfections in optical filter parameters. To ensure high channel isolation we need to inscribe FBG filters with complex apodization profiles. Changes in apodization profiles emerge in different filter bandwidth at -3 dB and -20 dB level and suppression of undesirable side lobes in optical filter amplitude response. Performance of three different apodization profiles and their influence on DWDM-direct systems main parameters: channel spacing and data transmission rate have been evaluated numerically.

2.1. Simulation method

To numerically evaluate impact of different FBG apodization profiles on high speed DWDM-direct system combination of two different simulation programs was used: Bragg Grating Filters Synthesis 2.6 (BGFS 2.6) simulation program for mathematical description of FBG optical filter and OptSim 5.2 simulation program to simulate high speed DWDM-direct systems. In the BGFS 2.6 simulation program different FBG optical filters with defined apodization profiles were realized. This simulation program is based on Transfer Matrix Method (TMM). TMM is used to create a numerical periodic non-uniform FBG filters. It is applied to solve the coupled mode equations and to obtain the spectral response of the fiber Bragg grating. In this approach, the grating is divided into uniform sections. Each section is represented by a 2x2 matrix. By multiplying these matrices, a global matrix that describes the whole grating is obtained (see Fig. 2. and equation 1):

Figure 2. Transfer matrix method used to obtain the spectral characteristics of a fiber Bragg grating (Δn - average index of refraction, Δz - section length, R_0, S_0, R_M, S_M - electromagnetic waves amplitudes)

$$\begin{cases} T_M = T_1 \cdot T_2 \cdot T_3 \cdot \ldots \cdot T_i, \\ \begin{bmatrix} R_M \\ S_M \end{bmatrix} = T_M \cdot \begin{bmatrix} R_0 \\ S_0 \end{bmatrix}. \end{cases} \quad (1)$$

The reflection coefficient of the entire grating is defined as:

$$\rho = \frac{S_0}{R_0}. \quad (2)$$

The main drawback of this method is that M may not be made arbitrarily large, since the coupled-mode theory approximations are not valid when uniform grating section is only a few grating periods long. Thus, it requires $\Delta z >> T$ [13, 14].

OptSim 5.2 simulation program uses method of calculation that is based on solving a complex set of differential equations, taking into account optical and electrical noise, linear and nonlinear effects. Two ways of calculation are possible: Frequency Domain Split Step (FDSS) and Time Domain Split Step (TDSS) methods. These methods differ in linear operator L calculations: FDSS does it in frequency domain, but TDSS calculates linear operator in the time domain by calculating the convolution product in sampled time. The first method is easy to realize, but it may cause severe errors during simulation. In our simulation we used the second method, TDSS, which despite its complexity grants a precise

result. The Split Step method is used in all commercial simulation tools to perform the integration of the fiber propagation equation:

$$\frac{\partial A(t,z)}{\partial z} = \{L + N\} A(t,z), \tag{3}$$

where $A(t,z)$-the optical field; L-linear operator that stands for dispersion and other linear effects; N – operator that is responsible for all nonlinear effects. The idea is to calculate the equation over small spans of fiber Δz by including either linear or nonlinear operator. For instance, on the first span Δz only linear effects are considered, on the second – only nonlinear, on the third – again only linear [15]. Us it is noticed before, in numerical investigation are used two simulation programs: BGFS 2.6 – to realize FBG filters amplitude and phase responses and OptSim 5.2 to numerically evaluate high speed DWDM-direct systems. Realized FBG filter parameters were recorded in data file, which after simple mathematical calculations were used in OptSim 5.2 simulation program to build user defined optical filters.

2.2. Simulation scheme and results

Simulation scheme (see Fig.3.) consists of transmitter, transmission line and receiver. Number of channels is chosen to evaluate influence of nonlinear optical effects (NOE): self – phase modulation (SPM), cross – phase modulation (XPM), four – wave – mixing (FWM) to used optical filters performance.

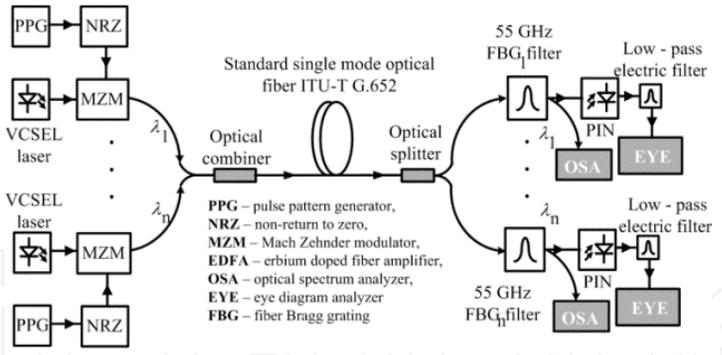

Figure 3. Simulation scheme for DWDM-direct transmission realization with FBG optical filters

The transmitter consists of pseudo-random data source with 2^{31}-1 bit sequence, non return to zero (NRZ) code former, continuous wavelength (CW) laser source and $LiNbO_3$-based external Mach Zehnder modulator (MZM). The data source produces a pseudo-random electrical signal, which represents the information we want to transmit via optical fibre. Then we use a code former to form NRZ code from incoming pseudo-random bit sequence. The NRZ has long been the dominant code format in fibre optical transmission systems, because of a relatively low electrical bandwidth for the transmitters and receivers and its insensitivity to the laser phase noise [16]. The optical pulses are obtained by modulating CW laser irradiation in MZM with previously mentioned bit sequence. Then formed optical

pulses are sent directly to a different length standard single mode fibre (SSMF). The utilized fibre has a large core effective area 80 μm², attenuation α = 0.2 dB/km, nonlinear refractive coefficient $n_k = 2.5 \cdot 10^{-20}$ cm/W and dispersion 16 ps/nm/km at the reference wavelength λ = 1550 nm. Receiver block consists of optical filter, PIN photodiode (typical sensitivity -17 dBm) and Bessel – Thomson electrical filter (4 poles, 7.5 GHz -3dB bandwidth). To simulate insertion loss (polarization dependent loss: 0.1 dB, ripple insertion loss: 0.2 dB, splice and connector loss: 0.1dB) of optical filter we used optical attenuator.

The main idea of our simulations is to demonstrate FBG filters with different apodization profiles (see Fig. 4.) influence on high speed dense WDM communication systems. Investigation of high performance optical band-pass filters are groundwork for realization of high speed dense WDM communication systems.

The main problem is to ensure high channel isolation between adjacent channels. To realize channel isolation performance evaluation of FBG optical filter we used eye diagram, bit error rate (BER) and optical signal spectrum in different system configurations (different channel spacing and data transmission speed). We have chosen three different apodization profiles (see Fig.4.): rectangular, cosinusoidal and Gaussian, four channel spacing values: 200 GHz, 100 GHz, 50 GHz and 25 GHz and two data transmission speeds: 2.5 Gbit/s and 10. 3125 Gbit/s.

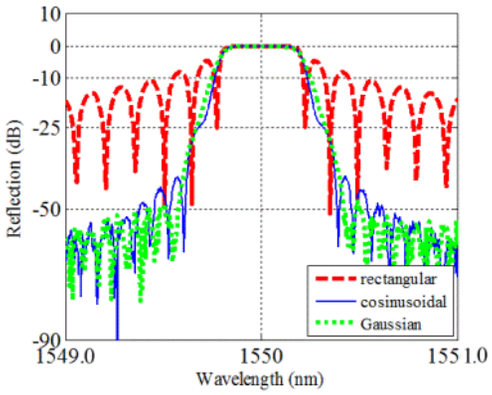

Figure 4. Amplitude response of 55 GHz FBG optical filters with different apodization profiles shown in inset

The results of BER dependence on channel spacing using FBG with rectangular, cosinusoidal and Gaussian apodization profiles are presented in Fig. 5. As we can see systems with 2.5 Gbit/s data transmission speed performance is better (BER values are lower) than systems with 10. 3125 Gbit/s data transmission speed. This can be explained by greater influence of chromatic dispersion on higher data transmission speed optical pulses. In addition, from results we can see that BER values are higher at 25 GHz channel spacing due to greater NOE influence and crosstalk. At both data transmission speeds and all channel spacing values, the worst performance showed the FBG optical filter with rectangular apodization profile. This is mainly because of great undesirable side lobes in optical filter amplitude response. These imperfections in filter amplitude response reduced channel isolation.

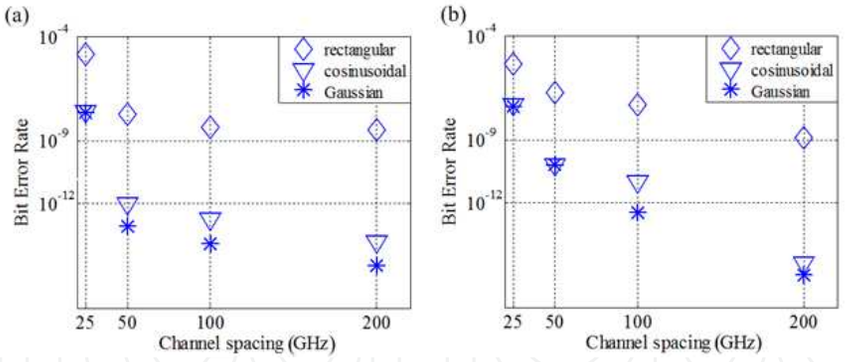

Figure 5. BER dependence on channel spacing using FBG with rectangular, cosinusoidal and Gaussian apodization profiles: a – 2.5 Gbit/s; b – 10.3125 Gbit/s data transmission speed. BER values measured at the worst channel.

As one could see from simulation results the influence of FBG filters with different apodization profiles on high speed DWDM-direct systems is enormous. To ensure high channel isolation and thus realize systems high performance FBG filter must be used with cosinusoidal or Gaussian apodization function because of narrow bandwidth at -20 dB level. FBG with rectangular apodization profile showed the worst performance which resulted in whole system degradation because of imperfections (great side lobes) in amplitude response.

3. Fiber Bragg grating characterization methods

Optical filters in optical transmission systems are a special subgroup of physical components defined in such a way that they select or modify parts of the spectrum of the signal [17, 18]. Signals and physical components can be expressed mathematically by complex functions describing amplitude and phase [17]. Amplitude transfer function describes loss dependency as function of wavelength for optical filter, but phase transfer function is responsible for introduced wavelength dependent amount of delay. There are different methods for transfer funtion characterization. Focus is related to the techniques which are for evaluation of phase transfer funtion and its related paremeters.

3.1. Jones matrix eigenanalysis

Polarization mode dispersion (PMD) decreases transmission systems bandwidth and is a fundamental parameter of both: optical fiber and passive optical components. The difference between group delays for two principle states of polarization (PSP) is the differential group delay (DGD) [19]. The PMD value is the average of DGD values. DGD varies randomly with wavelength and time which stands for dispersive effects. Moreover a second-order effect of PMD can lead to optical pulses length changes [20]. As a consequence an optical component with birefringence devoid of chromatic dispersion (CD), can exhibit optical pulses length changes owing to the second-order effects of PMD [21]. PMD is characterized by a Jones Matrix as a function of wavelength [22]. Jones Matrix is common to represent the polarization state of an optical signal or the transfer matrix of a passive optical device. The transfer matrix of an optical device specifies the relationship between the input and output

Jones vectors of the optical signal [20]. This transfer matrix can be characterized by measuring three output Jones vectors in response to three known input Jones vectors. It is worthwhile to note that although it is measured with a few specific polarization states of the optical signal, a Jones Matrix describes a passive optical device such as an optical filter and is independent of the input launching condition of the optical signal [22]. Two basic equations for this DGD estimation are given below. Thus, the two Eigen-values can be calculated from the products of Jones Matrix employing (4).

$$\rho_{1,2} = \frac{m_{11} + m_{22}}{2} \pm \sqrt{(\frac{m_{11} + m_{22}}{2})^2 - m_{11} \cdot m_{22} + m_{12} \cdot m_{21}} \quad (4)$$

Where $\rho_{1,2}$ is Eigen-values and m_{11}, m_{12}, m_{21}, m_{22} - products of Jones Matrix [22]. Therefore DGD can be expressed as the group delay difference as the function of the optical frequency:

$$\Delta\tau(\omega) = \left|\tau_{g1} - \tau_{g2}\right| = \left|\frac{Arg(\rho_1 / \rho_2)}{\Delta\omega}\right| \quad (5)$$

Where, τ_{g1} and τ_{g2} is group delays for two principle states of polarization, $Arg(\rho_1 / \rho_2)$ denotes the phase angle of ρ_1 / ρ_2 [22]. Equation (5) shows the principle of Jones Matrix technique for DGD measurement. An important practical issue is to choose the frequency step size $\Delta\omega$ for the measurement. For a small step size the measurement would take a long time and instability of devices would have strong impact on the results. For a big step size the output optical signal state of polarization would rotate for more than 45^o over each frequency step which leads to inaccurate results [19].

The Jones Matrix technique has a number of advantages compared to other DGD measurement methods [21]. First, it needs only a small wavelength window to perform a measurement. From this point of view method is more suitable for evaluation of detailed wavelength dependency of DGD and PMD. Second, Jones Matrix measurement can be made fast using automated procedures of polarization controller and a polarimeter. Third, the accuracy of the Jones Matrix technique is considered the best compared to other techniques [22]. Therefore Jones matrix Eigen-analysis (JME) is a measurement technique for accurately measure the DGD and PMD of any passive optical component [19].

In this research N7788B component analyser of Agilent Technologies was utilized to perform measurements of FBG with 55 GHz full width half maximum (FWHM) bandwidth. This technology is based on the JME which is the standard method for measuring DGD and PMD of passive optical devices [23].

Measurement scheme (see Fig.6) consists of $LiNbO_3$ polarization controller, polarimeter, tunable laser source and device under test (DUT): FBG with 55 GHz FWHM bandwidth.

Fig.7 shows measured amplitude transfer function and DGD as function of wavelength for FBG with 55 GHz FWHM bandwidth. Results show that DGD value within filters pass-band does not exceed 70 picoseconds.

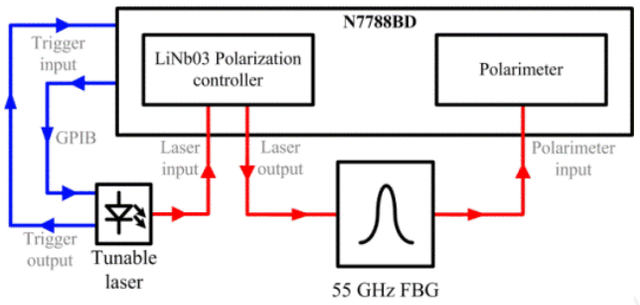

Figure 6. DGD measurement scheme [24]

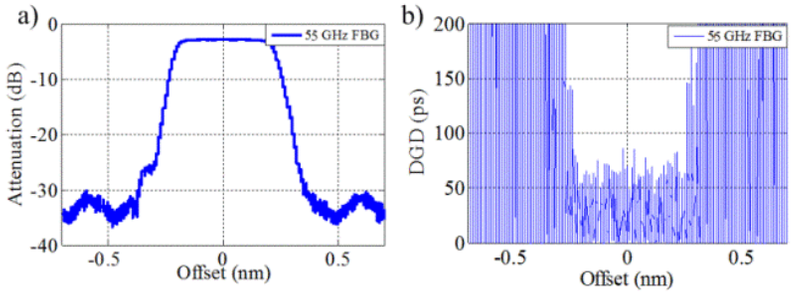

Figure 7. Measured amplitude transfer (a) function and differential group delay (b) of 55 GHz FBG

DGD and PMD value increases at the edges of the optical filter amplitude transfer function which could be a degradation factor for optical signal transmitted through device [25]. Therefore the relative bandwidth available to each broadband access systems channel is reduced, meaning that the channel experiences the effect of the edge of the pass-band of the filter transfer function, where the dispersion effects is expected to be most significant [17].

3.2. Modulation phase shift method

Agilent Technologies 86038B photonic dispersion and loss analyzer was employed for 55 GHz FBG filter parameters evaluation and numerous parameters were obtained: attenuation, group delay (GD) and chromatic dispersion as functions of wavelength. Test equipment is based on the modulation phase shift (MPS) method. In the conventional MPS method, light from a sinusoidal source is intensity modulated before being launched into the device under test [24]. MPS method obtains the group delay response of a device under test by measuring the change in phase of a sinusoidal radio frequency (RF) modulation envelope as the wavelength is changed [23].

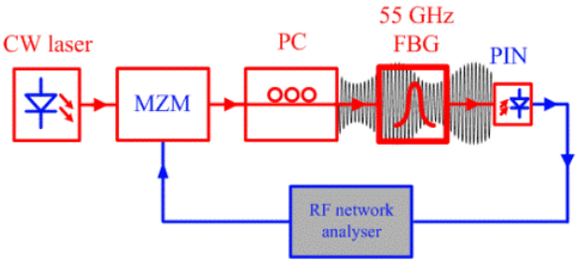

Figure 8. MPS method scheme for 55 GHz FBG measurements

See MPS method realization in Fig.8. The optical light source is a tunable distributed feedback laser. Light from a laser is sent to external MZM and is amplitude modulated (typically in the 100 MHz to 1.25 GHz range). After propagating through the DUT, the transmitted signal is detected by a PIN photodiode. A RF network analyzer is employed to provide a modulating signal of frequency f_m and to measure electrical phase difference between input and output signals [26, 27]. In practice, the wavelength is swept and the change in the group delay $\Delta\tau$ for each wavelength increment is calculated from the measured change in phase according to (6):

$$\Delta\tau_{(\Delta\lambda)} = -\frac{\Delta\varphi}{360^o} \cdot \frac{1}{f_m}. \tag{6}$$

Where the first factor is defined as the fractional cycle of RF phase shift and the second factor represents the period of the RF signal. The subscript $\Delta\lambda$ indicates that the change in group delay being measured was produced in response to an incremental change in wavelength. In (6) we can notice how the group delay and the measured electrical phase present opposite slopes [20, 27].

The attribute called dispersion is defined by:

$$D = \frac{\Delta\tau}{\Delta\lambda} \tag{7}$$

Where $\Delta\tau$ is the change in group delay in seconds corresponding to a change in wavelength $\Delta\lambda$ in meters. In real world applications, the dispersion parameter is given in units of picoseconds per nanometer. Combining (6) and (7), we obtain:

$$\Delta\varphi = -360^o \cdot D \cdot \Delta\lambda \cdot f_m \tag{8}$$

Equation (8) specifies that the amount of phase change obtained in response to a wavelength step is the product of total device dispersion, wavelength step and modulation frequency. This equation provides several key insights into the capabilities of the MPS measurement method. In order to achieve accurate measures it is important to have a stable wavelength step size, which completely depends on the tunable laser stability [20, 27].

Fig. 9 shows measured attenuation, GD and CD as function of wavelength for FBG with 55 GHz FWHM bandwidth. The insertion loss is 5,3 dB while its bandwidth at -1 dB level is 50 GHz and its bandwidth at -20 dB level is equal to 75 GHz. The group delay variation is limited to 50 ps in the pass-band and the dispersion at the center wavelength is equal to 0 ps/nm. The maximum dispersion in the bandwidth at -3 dB level is found to be within the range of -500 ps/nm to 500 ps/nm.

3.3. Efficient bandwidth measurement method

The main idea of our experiments is to evaluate efficient bandwidth of FBG with 55 GHz FWHM bandwidth. Efficient bandwidth of passive device provides limitations which are

required to take into consideration for realization of DWDM-direct transmission system for broadband access.

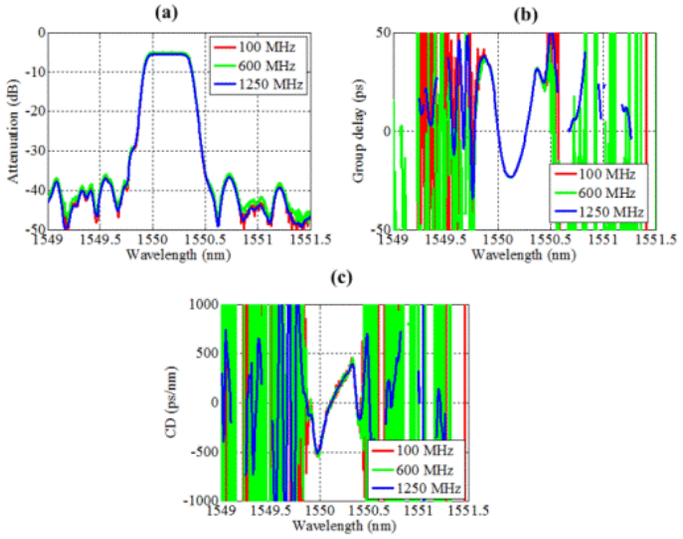

Figure 9. Measured attenuation (a), group delay (b), chromatic dispersion (c) and differential group delay (d) as function of wavelength for 55 GHz FBG filter

3.3.1. Method setup

Efficient bandwidth measurement scheme (see Fig. 10) was realized to investigate FBG with 55 GHz FWHM bandwidth with 2 GE and 10 GE optical signals. The efficient bandwidth measurement scheme consists of typical optical transmission system elements. The transmitter consists of pseudo-random data generator with 2^{31}-1 bit sequence, non-return to zero code former, continuous wavelength laser source and $LiNbO_3$-based external Mach Zehnder modulator.

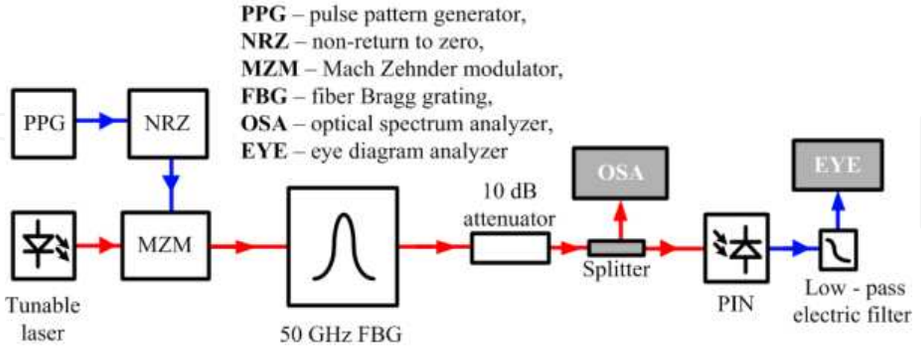

Figure 10. Efficient bandwidth measurement scheme

The data source produces a pseudo-random electrical signal, which represents the information. Then a code former is used to form NRZ code from incoming pseudo-random bit sequence. The optical pulses are obtained by modulating CW laser irradiation in MZM. Formed optical pulses are sent directly to a DUT at different CW laser central wavelength offset values. Receiver block consists of optical attenuator, PIN photodiode and Bessel –

Thomson electrical filter (4 poles, 7.5 GHz -3dB bandwidth). Attenuator with 10 dB rated value was used to simulate loss of 20 km optical fiber, splicing and connectors in direct access systems. Oscilloscope and optical spectrum analyser (OSA) was used to perform measurements of eye diagram and optical power spectral densities, accordingly.

3.3.2. Results for 2.5 GE and 10 GE transmission speed

The bit error rate measurement is a simple method for systems performance evaluation. The error counting in a practical system for realistically low BER values (< 10^{-12}) can be a long process. Therefore the International Telecommunications union (ITU) has created the eye diagram masks for different bit rates with a definite BER value [28].

Fig. 11 shows the eye diagrams and optical power spectral densities of 2 GE optical signals after FBG with 55 GHz FWHM bandwidth for different laser central wavelength offset values (-0.2 nm, -0.1 nm, 0 nm, 0.1 nm, 0.2 nm). Offset value was changed within FBG device pass-band with 0.1 nm step. This value was chosen to fit DWDM systems wavelength grid defined in ITU-T G.694.1 recommendation. As we can see from results greater optical signal amplitude and phase distortions are at the edges of the band-pass optical filter. On Fig.11.a and Fig.11.e are shown eye diagrams for -0.2 nm and +0.2 nm offset values and there are signal waveform degradation. From these results FBG efficient bandwidth is 0.4 nm or 50 GHz and is the same as FWHM bandwidth.

Fig. 12 depicts out the eye diagrams and optical power spectral densities of 10 GE optical signals after FBG with 55 GHz FWHM bandwidth for different laser central wavelength offset values (same as in Fig. 11). On Fig.5.a and Fig.5.e are shown eye diagrams for -0.2 nm and +0.2 nm offset values and there are signal and mask crossing which means that defined BER value is exceeded. The results show that efficient bandwidth is 0.2 nm or 25 GHz and is 0.2 nm or 25 GHz lower than FWHM bandwidth for this transmission speed.

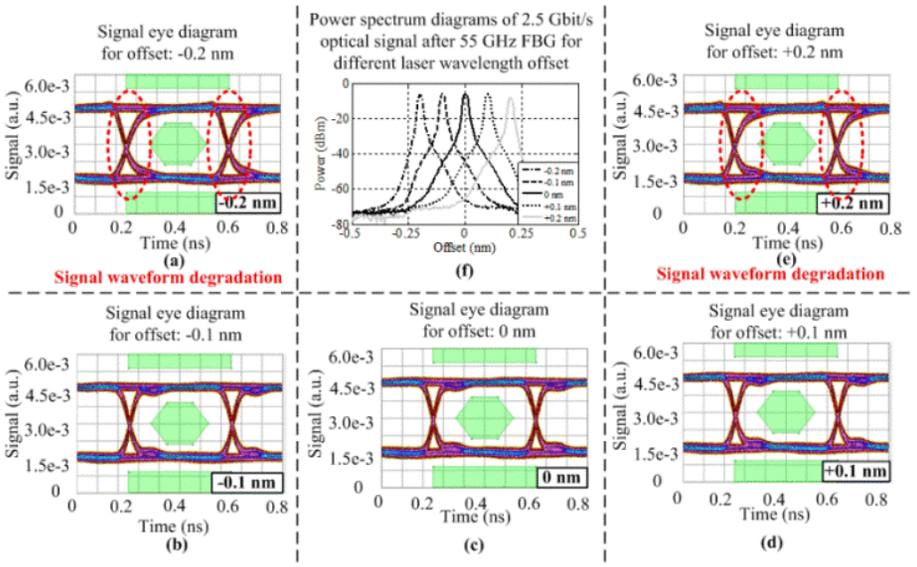

Figure 11. Eye diagrams (a-e) and optical power spectral densities (f) of 2GE optical signal after FBG with 55 GHz FWHM bandwidth for different CW laser wavelength offset shown in inset

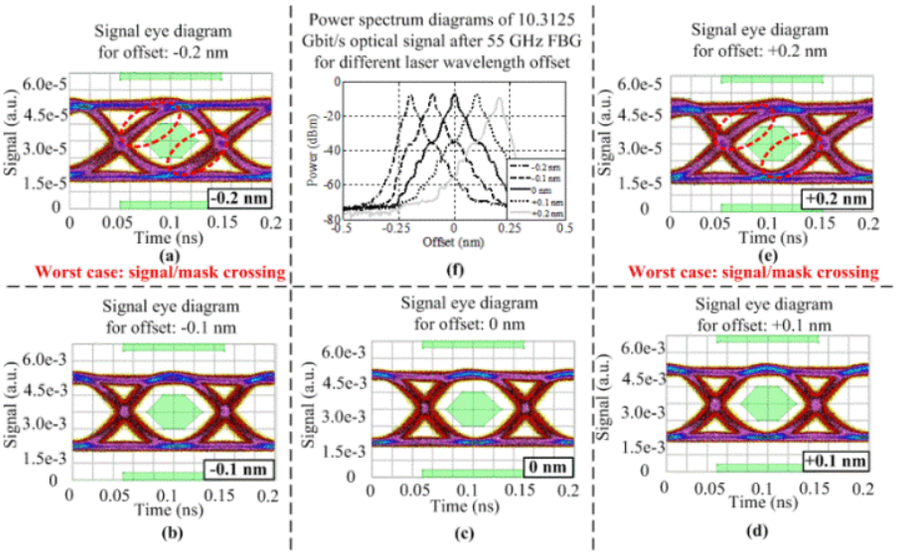

Figure 12. Eye diagrams (a-e) and optical power spectral densities (f) of 10GE optical signal after FBG with 55 GHz FWHM bandwidth for different CW laser wavelength offset shown in inset

4. Realization of new generation access system

Optical band-pass filter performance must be evaluated to increase spectral efficiency of overall optical transmission system [8]. Due to this, detailed investigation has been done into the FBG filter influence on the optical signals in DWDM-direct. For this purpose we have created the DWDM-direct measurement scheme and determined minimal channel interval for 55 GHz FBG filter at which the bit error ratio is sufficiently low. This evaluation was carried out employing eye diagrams and optical power spectral densities of the received optical signal.

4.1. Measurement setup

DWDM-direct scheme (see Fig. 13) is composed of three parts: a transmitter, an optical fiber, and a receiver. The transmitter consists of a pseudo-random data source with 2^{31}-1 bit sequence (Anritsu MU181020A), a non-return-to-zero code former (Anritsu MU181020A), a tunable continuous wavelength laser source (Agilent 81989A, 81949A), and an Avanex LiNbO3-based external MZM. The data source generates a pseudo-random electrical signal which contains the information to be transmitted via optical fiber. Then a code former is used to form an NRZ code from the incoming pseudo-random bit sequence. The optical pulses are obtained by modulating CW laser light in MZM with the generated bit sequence. After optical modulation the formed optical pulses are sent directly to a 20 km SSMF (G.652.d). The utilized fiber has a large core effective area of 80 μm^2, attenuation α = 0.2 dB/km, nonlinear refractive coefficient $n_k = 2.5 \cdot 10^{-20}$ cm/W, and dispersion 16 ps/nm/km at the reference wavelength λ = 1550 nm. The receiver block consists of an optical filter (55 GHz FBG), a PIN photodiode, and a Bessel–Thomson's electrical filter (4 poles, 7.5 GHz -3dB bandwidth, Anritsu MP1026A) [16].

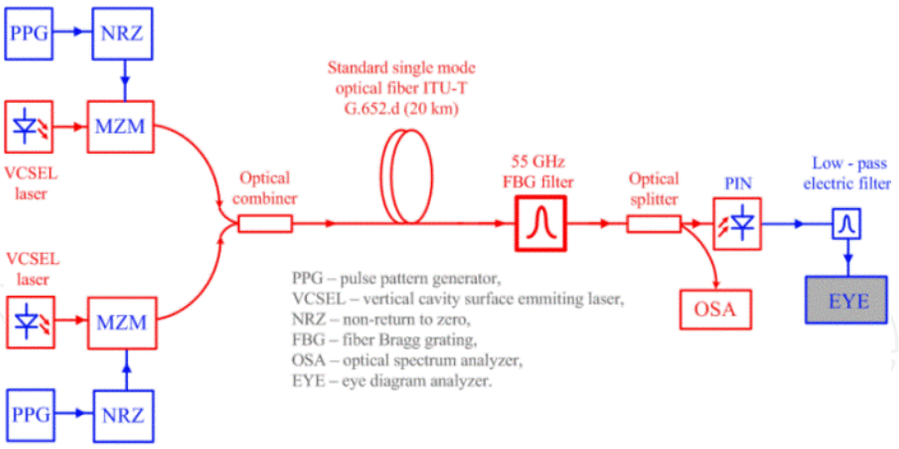

Figure 13. Realized DWDM– direct system for broadband access

In this research the minimal channel interval for DWDM-direct systems with 55 GHz FBG filter has been determined employing measured eye diagrams an optical power spectrum densities. A high-frequency oscilloscope Anritsu MP1026A was used to perform the eye diagram measurements and the optical spectrum analyzer ADVANTEST Q8384 was employed to get optical power spectral densities.

4.2. Spectral efficiency enlargement

Fig. 14 shows the eye diagrams and optical power spectral densities of a 2.5 Gbit/s DWDM-direct system realized with 55 GHz FBG after 20 km of SSMF for different channel intervals from 25 GHz to 125 GHz with 25 GHz (0.2 nm in a wavelength range) step. The step value was chosen to fit DWDM wavelength grid defined in ITU-T G.694.1 recommendation. Both signal detection in the 2.5 Gbit/s DWDM system, 55 GHz FBG, was observed with a 25 GHz channel interval. To reduce undesirable adjacent signal, the channel interval was increased, which gave lower BER values for the detected signal. As a result, the adjacent channel was suppressed more efficiently, because the steepness of a 55 GHz FBG device is very good and the adjacent channel's isolation is ~35 dB. As one can see from the results (Fig. 14b), a 50 GHz channel interval is sufficient to ensure the appropriate BER value for adequate system's performance. The results for greater channel intervals (75 GHz, 100 GHz and 125 GHz, Fig. 14c–e) are also shown to demonstrate DWDM-direct system's stability in the employed spectral range.

The eye diagrams and optical power spectral densities of a 10 Gbit/s DWDM-direct system for broadband access after 20 km of SSMF for the same channel intervals as in the previous case are shown in Fig. 15. Due to a higher transmission speed, the optical power spectral density is broader, which results in stronger influence of CD on the signal quality. This leads to greater degradation of the optical signal, which emerges as a larger standard deviation and jitter for "0" and "1" levels in eye diagram. Similar to the above, a 50 GHz channel interval is sufficient to ensure the appropriate BER value for normal performance of the system at 10 Gbit/s transmission speed; the spectral efficiency is in this case improved from 0.18 bit/s/Hz to 0.2 bit/s/Hz.

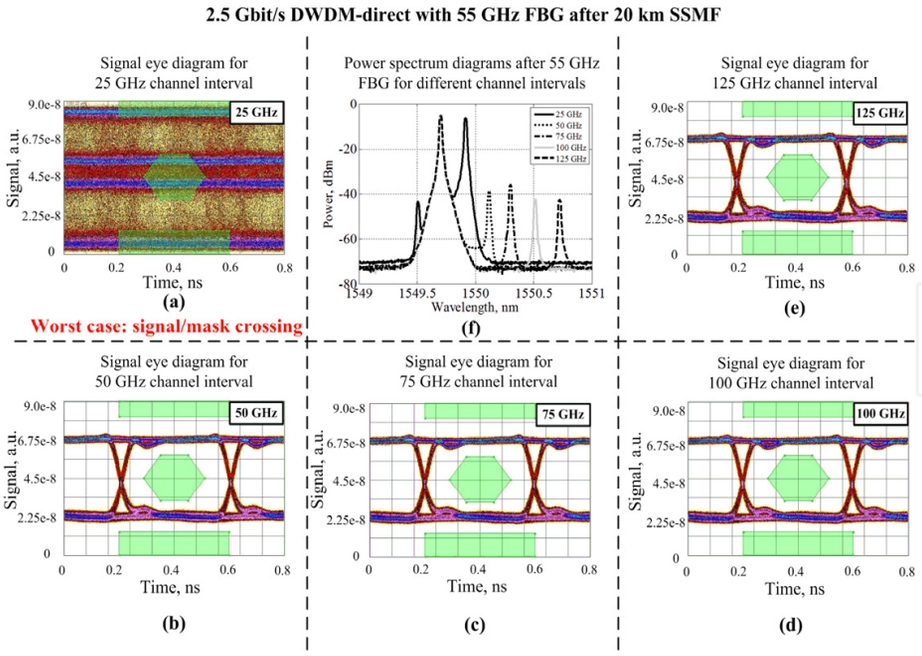

Figure 14. Eye diagrams (a–e) and optical power spectral densities (f) of 2.5 Gbit/s DWDM-direct system realized with a 55 GHz FBG after 20 km of SSMF for different channel intervals (shown in insets).

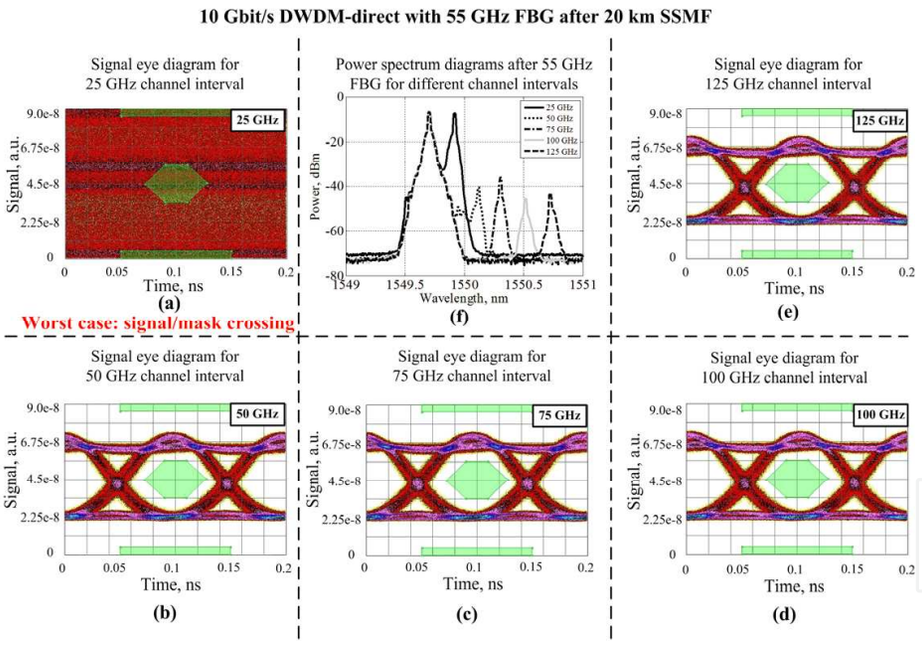

Figure 15. Eye diagrams (a–e) and optical power spectral densities (f) of 10 Gbit/s DWDM-direct system realized with a 55 GHz FBG after 20 km of SSMF for different channel intervals (shown in insets).

4.3. Channel number enlargement: numerical evaluation

Simulation scheme is shown in Fig. 3. Channel count of simulation scheme depends on simulation setup. Two, four and eight channels were chosen balancing between total capacity on one hand and physical limitations on the other.

The main idea of simulations is to demonstrate the possibility of channel number enlargement for FBG filter with 55 GHz FWHM bandwidth in DWDM-direct transmission system for broadband access.

Fig.16.a-c. depicts out power spectral densities and eye diagrams of 2.5 Gbit/s DWDM-direct transmission system with different channel count after 20 km of SSMF and Fig.16.d. shows BER dependence on distance for 50 GHz FBG. We can see that adjacent channel isolation value (~ 30 dB) for 55 GHz FBG is sufficient to realize reliable transmission at eight channel case. In this case influence of adjacent channel caused impairments is minimized by proper optical band-pass filter parameter selection.

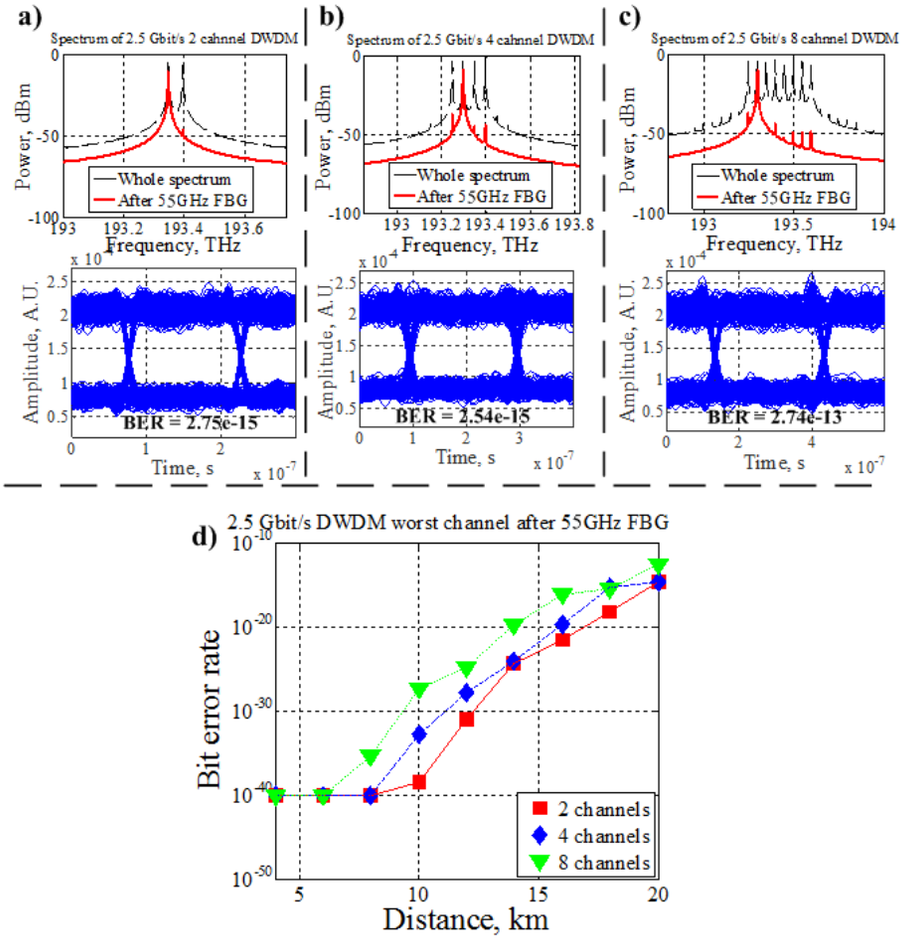

Figure 16. Power spectral densities and eye diagrams of 2.5 Gbit/s DWDM-direct a) two channels, b) four channels, c) eight channels system after 20 km of SSMF and d) BER vs. Distance with 55 GHz FBG optical filter. Results obtained at the worst channel.

Fig.17.a-c. depicts out power spectral densities and eye diagrams of 10 Gbit/s DWDM-direct transmission system with different channel count after 10 km of SSMF and Fig.17.d. shows BER dependence on distance for 55 GHz FBG. Transmission at higher data speed is more affected by chromatic dispersion of optical fibre and total power budget of system is reduced because of greater excess loss in MZM and lower receiver sensitivity for appropriate BER threshold.

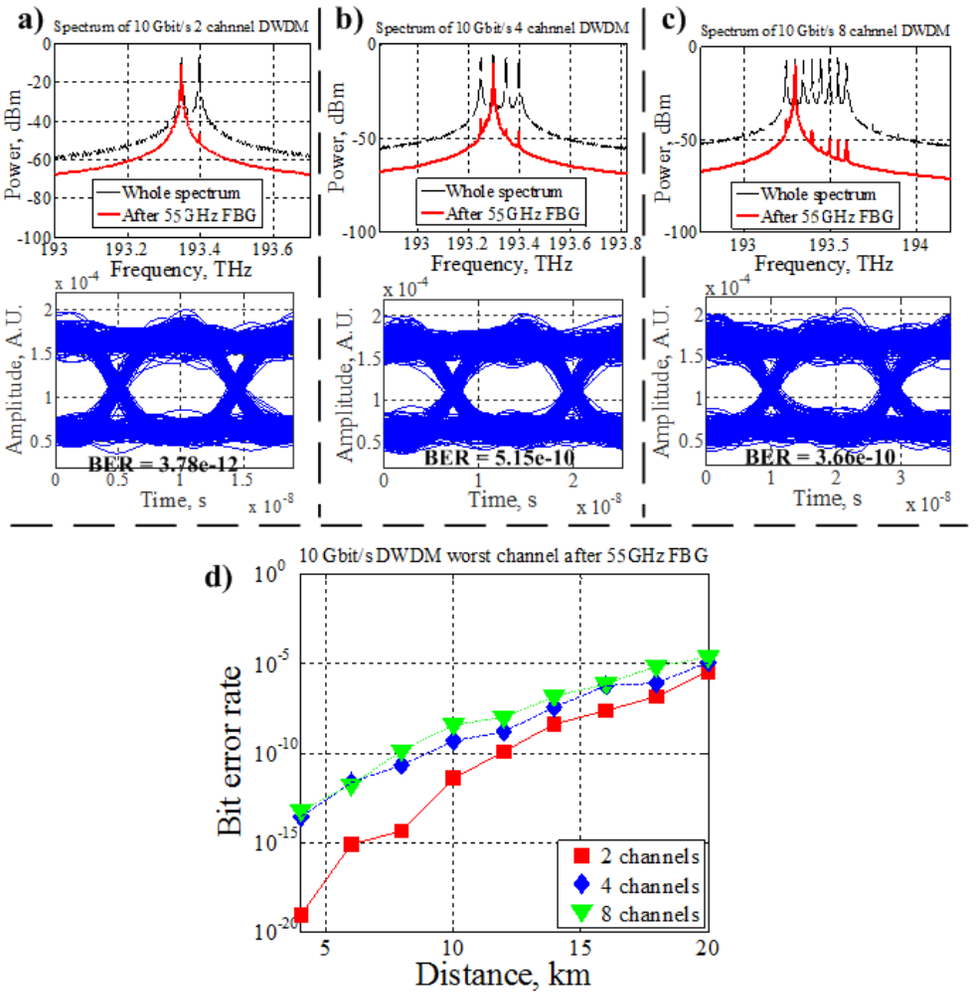

Figure 17. Power spectral densities and eye diagrams of 10 Gbit/s DWDM-direct a) two channels, b) four channels, c) eight channels system after 10 km of SSMF and d) BER vs. Distance with 55 GHz FBG optical filter. Results obtained at the worst channel.

5. Conclusions

As we can see from the results, the proper selection of optical filter amplitude transfer functions is of great importance. In this investigation influence of adjacent channel caused impairments is minimized by proper optical band-pass filter parameter selection. Reliable transmission is realized for 2.5 Gbit/s and 10 Gbit/s DWDM-direct with 55 GHz FBG for 20 km of SSMF.

Results show that DGD value within filters pass-band does not exceed 70 picoseconds for FBG with 50 GHz FWHM bandwidth. DGD value increases at the edges of the optical filter amplitude transfer function which could be a degradation factor for optical signal transmitted through device. Furthermore efficient bandwidth was evaluated for FBG devices employing optical signals with different transmission speed. Efficient bandwidth of 55 GHz FBG device was 0.4 nm or 50 GHz for 2GE optical signal and 0.2 nm or 25 GHz for 10GE optical signal.

We have realized a DWDM-direct system for broadband access that includes FBG filter with 55 GHz FWHM bandwidth. From the measurement results we found the minimal channel interval for the 55 GHz FBG to ensure reliable data transmission, and therefore were able to increase the spectral efficiency of the whole DWDM-direct system for broadband access. In 2.5 Gbit/s and 10 Gbit/s DWDM-direct systems with 55 GHz FBG the detection of both signals were observed for a 25 GHz channel interval. To achieve single-channel detection and suppression of the adjacent channel's power level the channel spacing was increased to 50 GHz. As a result the spectral efficiency of the 10 Gbit/s DWDM system with 55 GHz FBG was raised from 0.18 bit/s/Hz to 0.2 bit/s/Hz.

Author details

Oskars Ozolins, Vjaceslavs Bobrovs, Jurgis Porins and Girts Ivanovs
Riga Technical University, Telecommunications Institute, Latvia

Acknowledgment

This work has been supported by the European Regional Development Fund in Latvia within the project Nr. 2010/0270/2DP/2.1.1.1.0/10/APIA/VIAA/002.

6. References

[1] Kazovsky L. G., Shaw W.-T., Gutierrez D., Cheng N., and Wong S.-W. Next-Generation Optical Access Networks. Journal of Lightwave Technology 2007; 25(11) 3428-3442.
[2] Wong E. Next-Generation Broadband Access Networks and Technologies. Journal Of Lightwave Technology 2012 30(4) 597-608.
[3] Hecht J. Recycled Fiber Optics. How Old Ideas Drove New Technology. Optics and Photonics News 2012; 23(2) 22-29.
[4] Kataoka N., Wada N., Xu W., Cincotti G. and Kitayama K.-I. 10Gbps-Class, bandwidth-symmetric, OCDM-PON system using hybrid multi-port and SSFBG en/decoder. 14th Conference on Optical Network Design and Modeling (ONDM) 2010, March 15 2010.
[5] Effenberger F. J., Kani J., and Maeda Y. Standardization Trends and Prospective Views on the Next Generation of Broadband Optical Access Systems. IEEE Journal on Selected Areas in Communications 2010; 28(6) 773-780.
[6] Kehayas E. Designing Wavelength-Division-Multiplexed Optical Access Networks Using Reflective Photonic Components. 14th Conference on Optical Network Design and Modeling (ONDM) 2010, March 15 2010.
[7] Agrawal G. Nonlinear Fiber Optics (Third Edition). USA: Academic Press; 2001.
[8] Segarra J., Sales V. and Prat J. Agile Reconfigurable and Traffic Adapted All-Optical Access-Metro Networks" 11th International Conference on Transparent Optical Networks (ICTON) 2009, June 28 2009.

[9] Ozolins O., Bobrovs V., Ivanovs G. Efficient Bandwidth of 50 GHz Fiber Bragg Grating for New-Generation Optical Access. 19th Telecommunications forum TELFOR 2011, November 22-24, 2011.
[10] Miyazawa T., Harai H. Optical access architecture designs based on WDM-direct toward new generation networks. IEICE Transactions on Communications 2010; E93-B(2) 236-245.
[11] Pfennigbauer M., Winzer P. J. Choice of MUX/DEMUX filter characteristics for NRZ, RZ, and CSRZ DWDM systems. Journal of Lightwave Technology 2006; 24(4) 1689 – 1696.
[12] Shen Y., Lu K., and Gu W., Coherent and Incoherent Crosstalk in WDM Optical Networks Journal Of Lightwave Technology1999; 17(5) 759-764.
[13] Phing H.S., Ali J., Rahman R.A. and Tahir B.A. Fiber Bragg grating modeling, simulation and characteristics with different grating lengths. Journal of Fundamental Sciences 2007; 3(1) 167-175.
[14] Kashyap R. Fiber Bragg grating. USA: Academic Press; 1999.
[15] Bobrovs V., Ivanovs G. Parameter Evaluation of a Dense Optical Network. Electronics and Electrical Engineering 2006; 4(25) 33-37.
[16] Ozolins O., Bobrovs V., Ivanovs G. Efficient Wavelength Filters for DWDM Systems. Latvian Journal of Physics and Technical Sciences 2010; 6(1) 13–24.
[17] Venghaus H. Wavelength filters in fibre optics. Berlin: Springer; 2006.
[18] Azadeh M. Fiber Optic engineering. London: Springer; 2009.
[19] Chen L., Zhang Z., Bao X. Polarization dependent loss vector measurement in a system with polarization mode dispersion. Optical Fiber Technology 2006 12(1) 251–254.
[20] Hui R., O'Sullivan M. Fiber optic measurement techniques. Burlington: Elsevier; 2009.
[21] Haro J., Horche P.R. Evolution of PMD with the temperature on installed fiber Optical Fiber Technology 2008; 14(3) 203–213.
[22] Yao X. S., Chen X., Liu T. High accuracy polarization measurements using binary polarization rotators. Optics Express 2010; 18(7) 6667-6685.
[23] Kun X., Dai Y., Jin M., Jia F., Chen X., Li X., Xie S. A novel method of automatic polarization measurement and its application to the higher-order PMD measurement. Optics Communications 2003; 215(12) 309–314.
[24] Agilent Technologies. Agilent N7788B/BD optical component analyser. Agilent Technologies, Inc. 2008;11-6.
[25] Westhauser M., Finkenbusch M., Remmersmann C., Pachnicke S., Krummrich P. M. Optical Filter-Based Mitigation of Group Delay Ripple- and PMD- Related Penalties for High Capacity Metro Networks. Journal of Lightwave Technology 2011; 29(16) 2350 - 2357.
[26] Peucheret C. Fibre and component induced limitations in high capacity optical networks. PhD thesis, Technical University of Denmark; 2004.
[27] Agilent Technologies. Agilent 86038B Photonic Dispersion and Loss Analyzer, 2nd ed. Germany: Agilent Technologies Manufacturing GmbH; 2006.
[28] Ozolins O., Bobrovs V., Ivanovs G. DWDM Transmission Based on the Thin-Film Filter Technology. Latvian Journal of Physics and Technical Sciences 2011 3(5) 55–65.